Tanzania Journal of Forestry and Nature Conservation, Vol 90, No. 2 (2021) 27-40

EVALUATION OF LAND-USE AND LAND-COVER CHANGES CUM FOREST DEGRADATION IN SHASHA FOREST RESERVE, OSUN STATE, NIGERIA USING REMOTE SENSING

A.A. Adeyemi and H.A. Oyeleye

Department of Forest Resources Management,
Faculty of Agriculture, University of Ilorin, Ilorin, Nigeria

Corresponding Author: adeyemi.aa@unilorin.edu.ng

ABSTRACT

Sustainable forest management requires accurate information on forest covers and periodical changes. Availability and use of spatial data has become very helpful in x-raying structural changes in most tropical rain forest management options due to reliable accuracy of satellite images with readily-available image processing tools. Thus, we assessed forest drains and land-cover changes in Shasha Forest Reserve using Landsat TM, ETM+ and OLI/TC images acquired from USGS. The images were analyzed using ERDAS Imagine and Maximum Likelihood Algorithm in ArcGIS 10.5. Land-use/cover change-dynamics were characterized using Land Change Modeller. Classification accuracies were assessed using Kappa's and confusion matrix. Normalized Difference Vegetation Index analysis was performed in ArcGIS. The distinguished LULC were forest, farmland, built-up and water bodies/swamp. The forest cover and water bodies/swamp shrank by 638.91 and 1653.48 ha at -23.66 and -61.24 $hayr^{-1}$, respectively within the 27-year period. Meanwhile, farmlands and built-up areas increased by 1508.40 and 783.99 ha at 55.87 and 29.04 $hayr^{-1}$, respectively. Results further showed that the reserve was better-vegetated in 1991 (0.39) than 2018 (0.05). The major drivers of forest degradation in the area were subsistence agriculture, illegal timber exploitation and overexploitation of non-timber forest products. Overall classification accuracy was 95.1% with Kappa's coefficient of 0.9439. User's accuracy ranged between 90.8 and 96.2%, while Producer's accuracies were between 90.8 and 98.1%. The result of LULC change simulation showed that if the prevailing trends subsist without regeneration, and if other factors remained unchanged, forest and water bodies/swamp would dip further by -653.74 ha and -318.66 ha by 2050, while farmlands and built-up areas would increase by 622.62 ha and 349.78 ha, respectively, with potential negative consequences on environmental variables.

Keywords: Landsat images; land-use/cover changes; fragmentation; consistent forest losses.

INTRODUCTION

It will be impossible to separate the bond of interactions between man and the environment. As man uses the resources therein, there are negative consequences, which might take decades to repair. The resultant effects have been land-use and land cover changes with wide-ranging effects on both the culprit and the vulnerable. Since return to democratic governance in Nigeria, the country has witnessed monumental losses in its areas under forest covers, mostly by forest-dependent people. With poverty rate on the rise coupled with very uncertain political futures, governments are continually relaxing policies, which favoured biodiversity conservation in the past. At regional level, states have adopted measures perceived to boost industrial agriculture and promote internally-generated revenue. These measures are very inimical to forests and biodiversity conservation.

Consequently, most of the reserved and protected areas have been worse-hit, become fragmented, and eventually de-gazetted in favour of multinationals.

The use of remote sensing data is of immense value in characterizing and monitoring changes in vegetation patterns, deforestation and forest degradation (Li *et al*. 2017). Considering the palpable changes in most of the forest reserves in Nigeria, it is important to take advantage of remote sensing technologies to ascertain the extent and rate of natural forest conversion in the reserve. This will help to sustainably manage the forest biodiversity and preserve the state heritage (Juliev *et al*. 2019). Such information could fast-track focused decisions that would improve the conditions of the forest reserve.

In the past, Osun State was known to contain appreciable forest cover with many important economic trees like *Mansonia altissima*, *Milicia excels*, *Khaya grandifoliola* among several others in larger diameter categories, particularly Shasha Forest Reserve. It was reputed to be one of the richest remaining forests in south-west Nigeria due to its biological diversity and uniqueness. The reserve is, however, threatened by illegal logging, over-hunting and clearance for agriculture. This is evident in the 2004 data used by Olokeogun *et al*. (2014). Hitherto, little is known about the extent of forest degradation in the reserve. The only probable facts were that of farming and continued illegal exploitations, which were guessed to be negatively impacting the health of the reserve. However, there is dearth of sufficient data on forest degradation from which reliable conclusion can be drawn in order to formulate improved strategies for forest conservation.

Also, the rates of forest cover depletions in the past three decades are yet to be ascertained in the area. Therefore, we assessed land-use and land-cover changes in the reserve are assessed with a view to understanding forest degradation rate and profiling specific drivers of forest cover losses in the area. The study also involves simulation of possible future of the reserve should the current circumstances persist. Remote sensing and change detection studies predominantly focus on providing information on changing extents of and patterns of land-use and land-cover changes (Weng 2002). Effectiveness of Landsat TM, ETM+ and OLI/TC data for land-use/cover classification and change detection has variously been exemplified (e.g., Yuan *et al*. 2005, Kabba and Li 2011, Mussa *et al*. 2017, Othow *et al*. 2017, Bello *et al*. 2018, Jiménez *et al*. 2018, Adeyemi and Adeleke, 2020, Adeyemi and Ibrahim, 2020).

MATERIALS AND METHODS

Study Area

Shasha Forest Reserve (SFR) is located between latitudes 6°55'00" and 7°1'00"N longitudes 4°2'00" and 4°32'30"E in Osun State, south-west Nigeria (Figure 1). The reserve was first gazetted in 1925, as part of the Old Shasha Forest Reserve under an agreement with Ijebu Native Authority. It shares boundaries with Omo Forest Reserve in the west. The northern and eastern boundaries are with Ife Native Authority Reserve and Oluwa Forest Reserve in Ondo State. Shasha FR covers an area of 23,621.31 ha. Out of which about 1,559.8 ha are under forest plantations of exotic and indigenous tree species, including *Gmelina arborea*, *Tectona grandis*, *Pinus caribaea*, *Terminalia spp.* and *Nauclea diderichii*. The remaining 22,061.51 ha are now covered by pockets of fragmented natural forests.

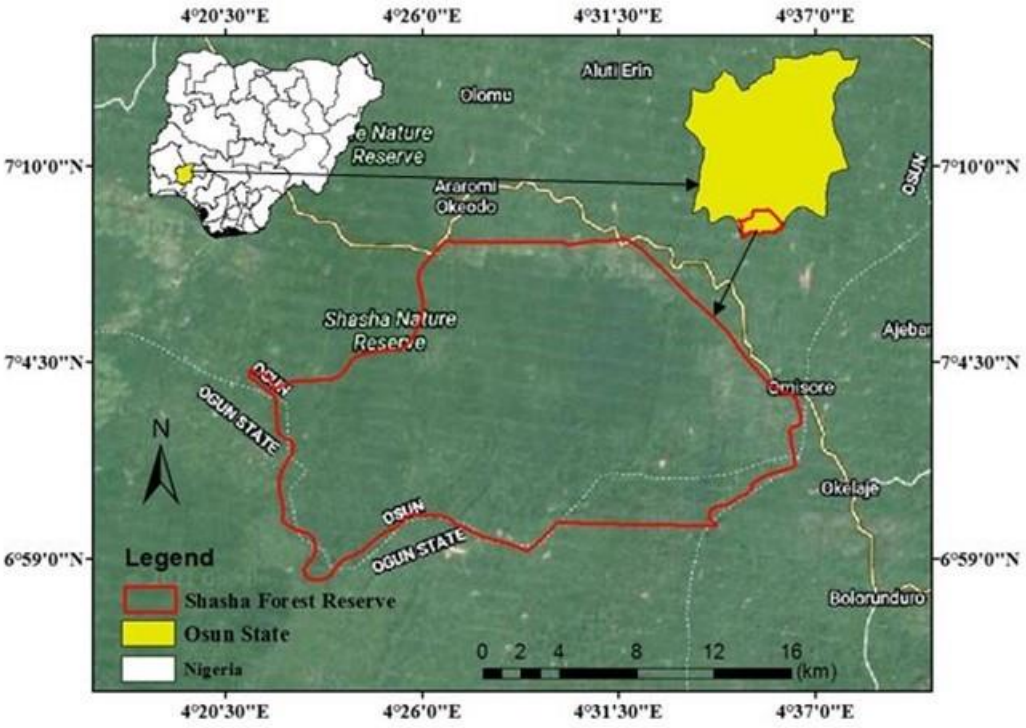

Figure 1: Map of Shasha Forest Reserve

Annual rainfall ranges between 887 mm and 2,180 mm. The mean annual temperature is about 26.5°C with annual range of between 19.5°C and 32.5°C. The rainy season in SFR usually commences from March/April and lasts till November. The original vegetation structure of Shasha Forest Reserve is multi-layered with scattered emergent. The reserve is subdivided into Area 4 and Area 5. The soils belong to the highly ferruginous tropical red soils associated with basement complex rocks. As a result of the dense humid forest cover in the area, the soils are generally deep and of two types, namely, deep clayey soils formed on low smooth hill crests and upper slopes, and the sandier hill wash soils on the lower slopes.

Image Datasets

The study involved the use of multi-temporal Landsat images for land-cover classification and change detection analysis. Landsat TM, ETM+ and OLI/TC satellite images of 4 age-series acquired from the United States Geological Survey (USGS) through Earth Explorer were used for the study (Figure 2). Among all the available satellite data, the scenes chosen are presented in Table 1. The satellite images were obtained during dry season for each year, between December and January (i.e. 1991, 2002, 2014 and 2018). Satellite images were selected to fall near anniversary windows to allow for comparison of vegetation phenology and minimises discrepancies in reflectance, which could result from seasonal variations in vegetation and water regimes, as well as differences in sun angle, as observed by Coppin *et al*. (2004). This choice of dry season in image selections was also guided by sensitivity to cloud cover, which could obscure terrain information in satellite scenes. The 1991, 2014 and 2018 images were geometrically corrected to a common Universal Transverse Mercator coordinate system, Datum WGS 1984; Zone 32N, based on a 1:50,000 topographic map scales with the 2002 image as the master. Each of the four image-types was resampled to produce region of interest (ROI), using the steps in subsequent sections.

For Landsat 8 OLI/TC of 2014 and 2018, Bands 5 (NIR): 0.85-0.88 µm, 4 (red): 0.64-0.67 µm and 3 (green): 0.53-0.59 µm were combined (stacked) together to form a single

multi-spectral image dataset using the following steps in ArcGIS 10.5:

Arctool Box
- ► Data Management Tools
- ► Raster
- ► Raster Processing
- ► Composite Bands
- ► Band Selection in this order
- ► 5,4,3
- ► OK
- ► Done.

For each Landsat image, the pre-processing operations performed consist of atmospheric correction, radiometric corrections and extraction of region of interest (i.e., the study area to be analyzed) or sub-setting, as follows:

Spatial Analyst Tools
- ► Extraction
- ► Extraction by Mask
- ► Input raster file
- ► (i.e., the composite image)
- ►Input feature mask (select the vector or enveloped file, as the case may be)
- ► Ok.

For Landsat 7 images, however, gap filling was done for each of the bands before band combination to remove scanline errors as follows:

ArcTool Box
- ► Landsat Toolbox
- ► Fix Landsat 7 Scanline Errors
- ► Ok
- ► done.

These procedures were repeated for Landsat 7 ETM+ image of 2002 using band combination 4,5,3 and 4,3,2 for Landsat 5 TM of 1991 image.

Image Pre-processing

The Landsat images were level-1 products, implying that they were already corrected for geometric accuracy by the data provider. However, to maximize the use of all spectral information contained in the satellite images, image pre-processing including atmospheric correction, radiometric calibration and image sub-setting performed in ERDAS Imagine 2014 Software. Prior to image classification, ground-truthing of relevant land-cover and land-use types within the study area was done. Field data were collected using Global Positioning System (GPS) Receiver for collection of coordinates at various locations within the study area. This involves the use of random points generated during first stage of image processing using Landsat 8 OLI/TC image of 2018 (prior to fieldwork).

Table 1: Characteristics of satellite images used for the study

Sensor	Band	Wavelength (µm)	Resolution	Year	Date
Landsat 5 (TM)	Band 1 - Blue	0.45 - 0.52	30	1991	05/01/1991
	Band 2 - Green	0.52 - 0.60	30		
	Band 3 - Red	0.63 - 0.69	30		
	Band 4 - NIR	0.76 - 0.90	30		
Landsat 7 (ETM+)	Band 1 - Blue	0.45 - 0.52	30	2002	03/01/2002
	Band 2 - Green	0.52 - 0.60	30		
	Band 3 - Red	0.63 - 0.69	30		
	Band 4 - NIR	0.77 - 0.90	30		
Landsat 8 OLI/TC	Band 2 - Blue	0.452 - 0.512	30	2014	30/12/2014
	Band 3 - Green	0.533 - 0.590	30		
	Band 4 - Red	0.636 - 0.673	30		
	Band 5 - NIR	0.851 - 0.879	30		
Landsat 8 OLI/TC	Band 2 - Blue	0.452 - 0.512	30	2018	04/01/2018
	Band 3 - Green	0.533 - 0.590	30		
	Band 4 - Red	0.636 - 0.673	30		
	Band 5 - NIR	0.851 - 0.879	30		

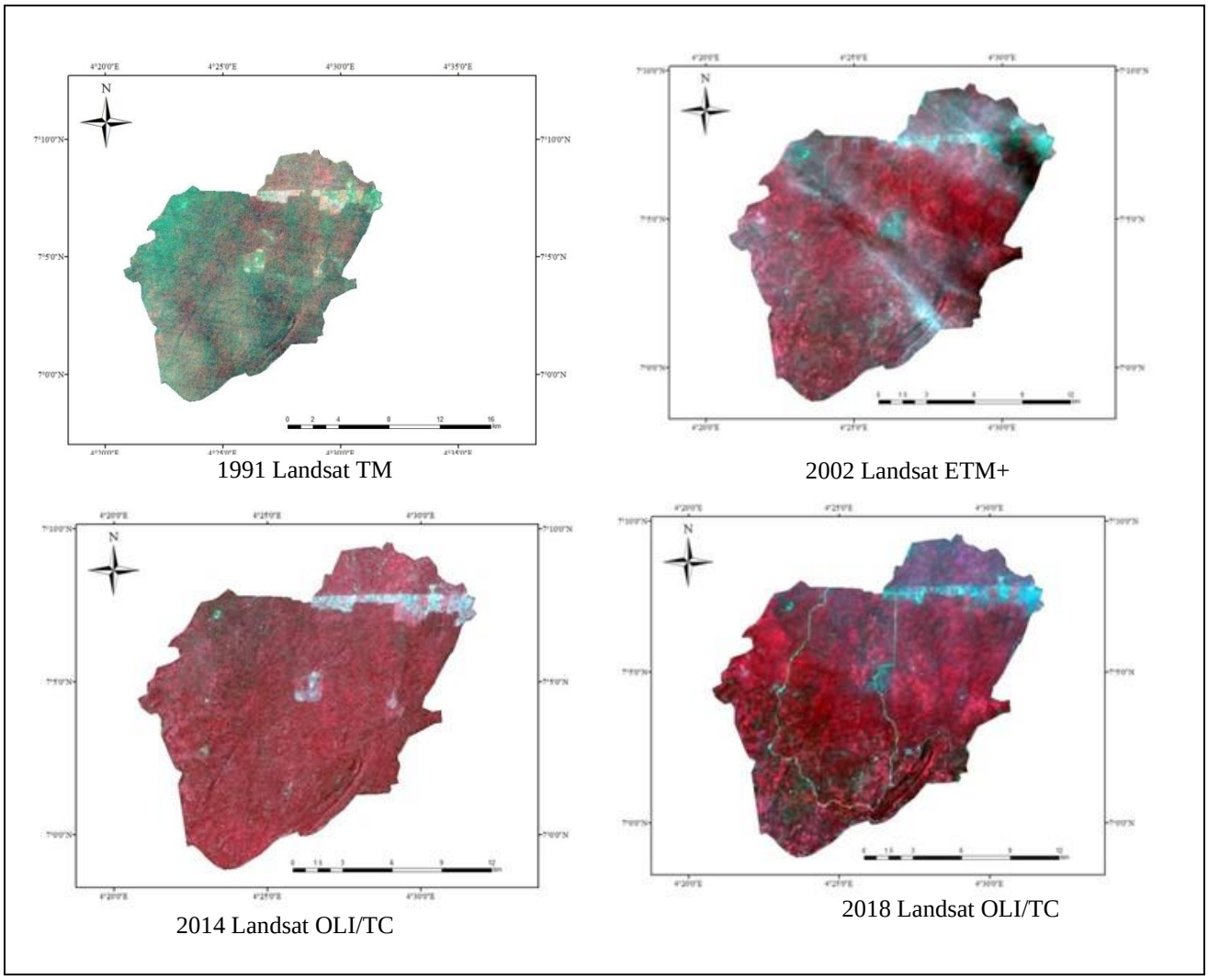

Figure 2: Extracted images of the study area for the four datasets

Image Analysis and LULC Classification

Supervised (maximum likelihood) classification method was adopted. The image pixels were grouped into finite classes based on their spectral signatures (land-cover classes). This was achieved using Maximum Likelihood Algorithm. Maximum likelihood classification (MLC) was preferred because it takes the variability of the classes into account by using the covariance matrix (Morgan *et al*. 2015; Ayele *et al*. 2018), and it is also the most-accurate algorithm in ERDAS Imagine. A total of four land-use and land-cover types were distinguished (i.e. forest, farmland, built-up area and water bodies/swamp). The accuracy assessment of the classified layers was done using independent training data collected during field surveys.

The dynamics of land-use and land-cover changes were analyzed using Land Change Modeler (LCM) by IDRISI (2014). The LCM tool was used to analyze changes in the forest landscape over four periods: 1991-2002, 2002-2014 and 2014-2018. The Land Change Modeler was adopted and applied for the Land-use/land-cover changes analysis due to its capacity to execute accurate automated decision support system. It simplifies the complexities of change analysis, and allow for rapid analysis of land-cover dynamics, enable the establishment of empirically modelled relationships to explanatory variables, and simulate future land change scenarios.

Vegetation Index

The Normalised Difference Vegetation Index (NDVI) is one of the oldest, well-

known, and most-frequently used VI. The combination of its normalized difference formulation and use of the highest absorption and reflectance regions of chlorophyll make it robust over a wide range of conditions. It was computed as:

$$NDVI = \frac{\rho NIR - \rho RED}{\rho NIR + \rho RED} \quad (1)$$

Where:

ρ_{NIR} and ρ_{RED} = reflectance at near infrared and red wavelength bands, respectively

Although NDVI values range between -1 and 1. The common range for green vegetation is 0.2 to 0.8. The NDVI was used to measure changes in green vegetation.

The Change Matrix

The first step in change detection was raster to vector conversion, as follows:

Arctool Box
- ► Conversion Tools
- ► From Raster
- ► Raster to Polygon
- ► Input Raster (include class in the attribute table of the raster data)
- ► Select the class created in the raster
- ► Ok
- ► done.

The second step was dissolution of the vector data (polygon). This was done following the steps:

Geoprocessing
- ► Dissolve (the 1988, 1999, 2002, 2013 and 2018 images done separately)
- ► Input feature class (select the vector file to be dissolved)
- ► Ok
- ► done.

The third step was unification or to unify the three images or datasets (1988, 1999, 2002, 2013 and 2018 images), as follows:

Geoprocessing
- ► Union
- ► Input feature class (select the three dissolved vector files for 1991, 2002, 2014 and 2018)
- ► Ok
- ► done.

Then open the attribute table of the unified vector (shapefile)
- ► Add another field (Area)
- ► right-click on the field
- ► Calculate Geometry
- ► Yes
- ► Change the unit to hectare
- ► Ok
- ► Yes
- ► Export the attribute table
- ► Table Options
- ► Export
- ► Change the file extension to dBASE Table
- ► Save
- ► OK
- ► No
- ► done.

The exported file was then opened in excel. The next thing was to make pivot table for the four years, and the differences in land-use/land-cover over the period was then determined using appropriate statistics. The determination of losses and trend analysis over 27-year period was obtained from the change matrix table. The net gains or losses to persistence ratio of each of the LULC types between 1991 and 2002, 2002 and 2014, 2014 and 2018 were determined. The mathematical computations were then done as follows:

Trend

$$\Delta LULC = L_2 - L_1 \quad (2)$$

Where:

L_2 (ha) = final year;
L_1 (ha) = initial year.

Rate of Change

$$R_t = \left((L_2 - L_1) \times \frac{1}{t}\right) \quad (3)$$

Where: t (year) = periodic interval

Projection

$$A_2 = \left(\left(R_t.t \times {}^{L_1}/_{100}\right) + L_1\right) \quad (4)$$

$$P_r = A_2 + R_i \quad (5)$$

Where:

P_r = predicted area increase;
A_2 = predicted year's trend,
L_1 = land-use/land-cover of base year (1991);
R_t = the rate of change of LULC in 28 years;

R_i = ratio increase; t = years of projection.

Classification Accuracy

The overall accuracy of land-use/land-cover classification was done by creating a confusion matrix in ArcMap 10.5 using ground reference points obtained during ground-truthing, and following these steps:

Spatial Analyst Tools
► Extraction
► Extract Multi Values to Points
► Input point features (input the Ground-truth GPS points collected on the field)
► Input raster (input the classified image)
► Ok
► done.

The attribute table was then exported (in dBASE format) for further analysis of the confusion matrix to determine classification accuracy and Kappa Coefficient. A total of 600 ground-truthed points (locations) were used for accuracy assessment of the land-use/land-cover classification. A total of 600 points were also created in the classified image of the study area to generate the cell array for confusion matrix table (as done by Adeyemi and Ibrahim (2020). Accuracy was computed by dividing the total correctly-classified pixels by the total number of pixels in the confusion matrix. Overall classification accuracy was then determined by:

$$Y = \frac{\sum_{i=1}^{n} x_i}{\sum_{j=1}^{N} X_j} \times 100 \quad (6)$$

Where:
Y = overall accuracy,
x_i = the i[th] correct point, X
$_j$ = total number of all points.

Other statistics used for accuracy assessment included sensitivity (producer's accuracy), specificity, commission error, omission error, users' accuracy and Kappa's coefficient (K) as follows:

$$Producer's\ Accuracy = \frac{w}{w+x} \quad (7)$$

$$User's\ Accuracy = \frac{y}{y+z} \quad (8)$$

$$Specificity = \frac{z}{x+z} \quad (9)$$

$$Commission\ Error = 1 - Specificity \quad (10)$$

$$Ommission\ Error = 1 - Producer's\ accuracy \quad (11)$$

Where:
w = number of times a classification agreed with the observed value;
x = number of times a point was wrongly classified;
y = number of times a point was correctly classified;
z = number of times a point was not classified as 'x' when it was not observed to be 'x'.

Kappa's coefficient measures perfect agreement between prediction and reality or classification results and the real observation, as is the case in this study. It was computed as:

$$K = \frac{N \sum_{ij=1}^{r} x_{ij} - \sum_{ij=1}^{r} (x_{ij} + Xx_{+1})}{N^2 \sum_{ij=1}^{r} (x_{ij}\, Xx_{+1})} \quad (12)$$

Where:
r = number of rows and columns in error matrix;
N = total number of observations (pixels);
x_{ij} = observations in the *ith* row and *jth* column;
x_{+i} = marginal total of the *ith* row;
x_{+j} = marginal total of the *jth* column.

Kappa Coefficient ranges between 0 and 1. A Kappa coefficient of 1 implies perfect agreement, while any value nearing zero means that the agreement between prediction and reality or between classification and real observation is no better than that due to chance.

RESULTS

Land-use and Land-cover Classes of Shasha Forest Reserve

The classification of the four (4) images in the age-series yielded land-cover maps of the study area and from these; four (4) LULC classes were identified. The characteristics of these land-cover types are described in Table 2.

Table 1: Description of different LULC categories

LULC	Description
Built-up area	Area densely covered by road, buildings and other infrastructure.
Farmland	Lands used for cultivation of subsistence and/or commercial agriculture.
Forest	Natural forest and artificial forest i.e. Plantation in the reserve.
Water bodies/Swamps	Main water bodies and wetlands that are forested in the study area.

LULC Status

Figure 3 presents the multi-temporal LULC with four major classes, viz: forest, farmland, built-up area and water bodies/swamps of 1991, 2002, 2008 and 2018. In 1991, forest occupied 19,042.38ha (80.6%). This was followed by water bodies/swamps with 3,574.89 ha, (15.1%), which was scattered around the north, south, east and the western parts of the area. Farmland covered 531.9 ha (2.3%) of the area, located mainly around the northern part of the reserve. Built-up areas were least with 472.14 ha (2.0%). In 2002, forest increased to 19,894.77 ha (84.2%), with concentration in most part of the reserve except in an area dominated by water bodies/swamps that occupied 1,653.21 ha (7.0%), less than 50% of its original extent. Farmland increased to 1,247.94 ha (5.3%), and built-up area also surged to, 825.39 ha (3.5%) with concentration within the region where people farm and very few scattered ones in other areas. In 2014, forest occupied 20,934.45ha (88.6%) with an increase of 4.4% in twelve years (from the previous period). Water bodies/swamps, however declined by 1.8% to 1,223.82ha (5.2%) within the same period. Farmland covered 843.93 ha (3.6%) representing a decline of 1.7% from previous period. Similarly, built-up area contrasted by 0.9% to 619.11 ha (2.6%). Between 2014 and 2018, forest sharply contrasted by 10.7% to 18,403.47 ha (77.9%) of the land area. Farmland gained 5.1% to occupy 2040.30 ha (8.7%) within the period. Water bodies/swamps was up by 2.9% with 1921.41 ha (8.1%). There was also an increase of 2.7% in built-up area at 1256.13 ha (5.3%) within that period (Figure 3).

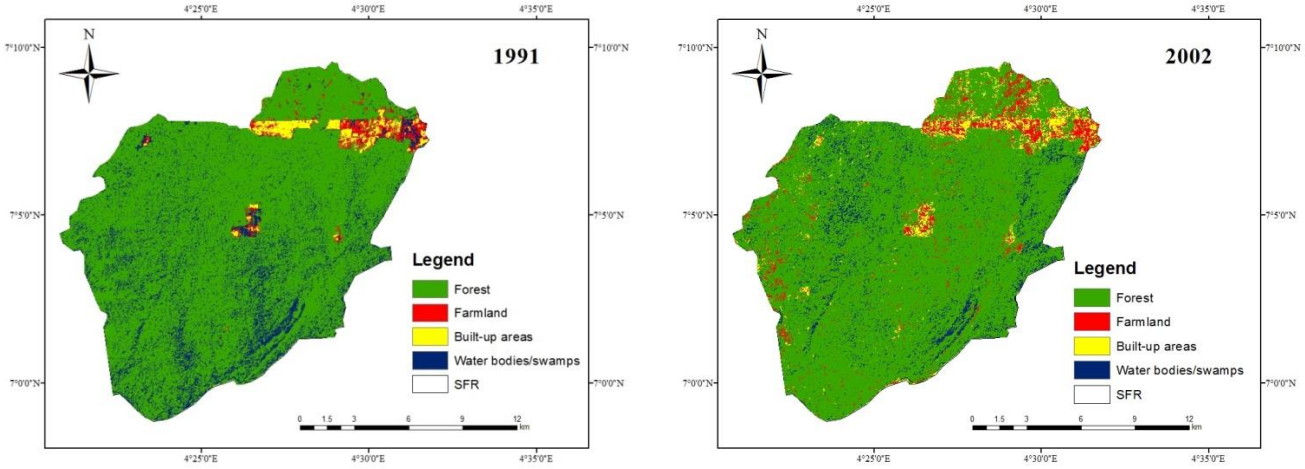

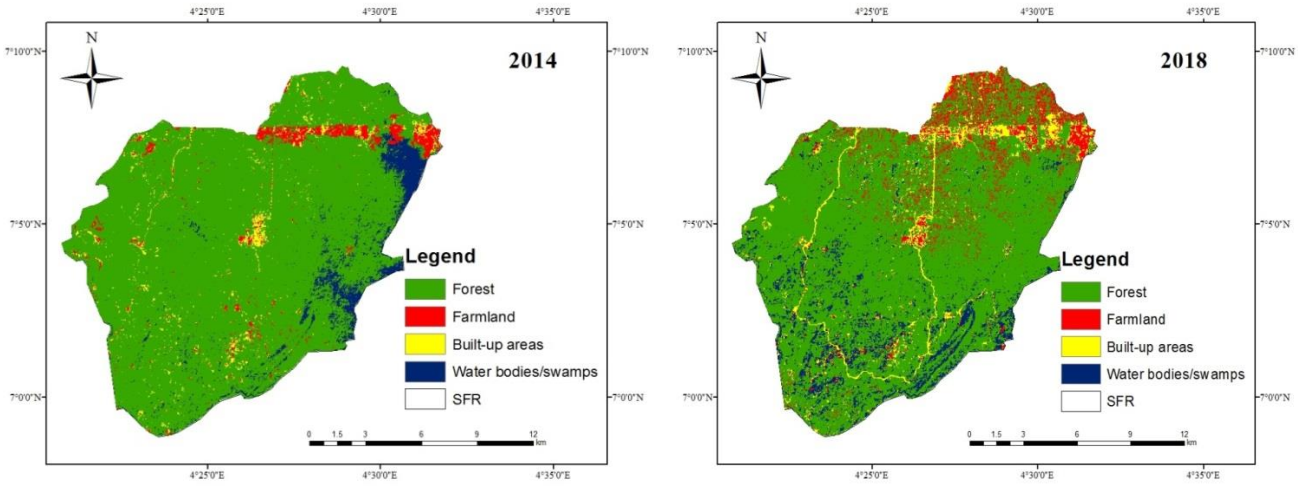

Figure 3: LULC change in Shasha Forest Reserve between 1991 and 2018

Land-use/Land-cover Change Trends in Shasha Forest Reserve between 1991 and 2018

The LULC changes between 1991 and 2018 in Shasha forest reserve are presented in Table 3. On the whole, forest decreased by 638.91 ha (2.7%) over the 27 years period. This translates to an annual loss of 23.66 ha. Farmland gained 1,508.4 ha (6.4%) in 27 years. This translates to an annual gain of 55.86 ha. Built-up areas increased by 783.99 ha (3.3%) between the assessment period at an annual gain of 29.04 ha. Nevertheless, water bodies/swamps shrank by 1653.48 ha (7.0%) at an annual loss of 61.24 ha. From 1991 to 2002, forest, farmland and built-up areas experienced a positive change of 852.39 ha (3.6%), 716.04 ha (3.0%), 353.25 ha (1.5%), respectively while water bodies/swamps experienced a decline of 1921.68 ha (8.1%). Between 2002 and 2014, forest has its area experiencing a positive change of 1039.68 ha (4.4%), while that of farmland, built-up areas and water bodies/swamps experienced negative changes of 404.01 ha (1.7%), 206.28 ha (0.9%), 429.39 ha (1.8%). From 2014 to 2018, however, forest experienced its most negative change of 2530.98 ha (10.7%), while farmland, built-up areas and water bodies/swamps were positively impacted with 1196.37 ha (5.1%), 637.02 ha (2.7%) and 697.59 ha (3.0%), respectively.

Table 3: Land-use and Land-cover change trend in SFR between 1991 and 2018

	Area extent				LULC change		Rate
	1991		2018		1991-2018		
LULC	Area (ha)	%	Area (ha)	%	Area (ha)	%	$hayr^{-1}$
Forest	19,042.38	80.6	18,403.47	77.9	-638.91	-2.7	-23.66
Farmland	531.90	2.3	2,040.30	8.6	1,508.40	6.4	55.87
Built-up areas	472.14	2.0	1,256.13	5.3	783.99	3.3	29.04
Water bodies/Swamps	3,574.89	15.1	1,921.41	8.1	-1,653.48	-7.0	-61.24

Normalized Difference Vegetation Index (NDVI)

Table 4 shows that the reserve was more vegetated in 1991 than any other period of assessment. The study shows that vegetation index decreased over the 27 years period from 0.38 in 1991 to 0.05 in 2018. The maximum NDVI (0.38) was found in 1991, which indicated an increase in vegetation. The lowest NDVI (0.05) was found in 2018,

indicating that other LULC types increased in that year to the detriment of forest vegetation cover. This ranged between 0.39 in 1991 to 0.05 in 2018. The NDVI value below zero i.e., in 2014 and 2018 indicated increases in water bodies/swamps (Figure 4).

Table 4: NDVI analysis result for Shasha Forest Reserve

Year	Minimum	Maximum
1991	0.12	0.38
2002	0.16	0.35
2014	-0.19	0.08
2018	-0.08	0.05

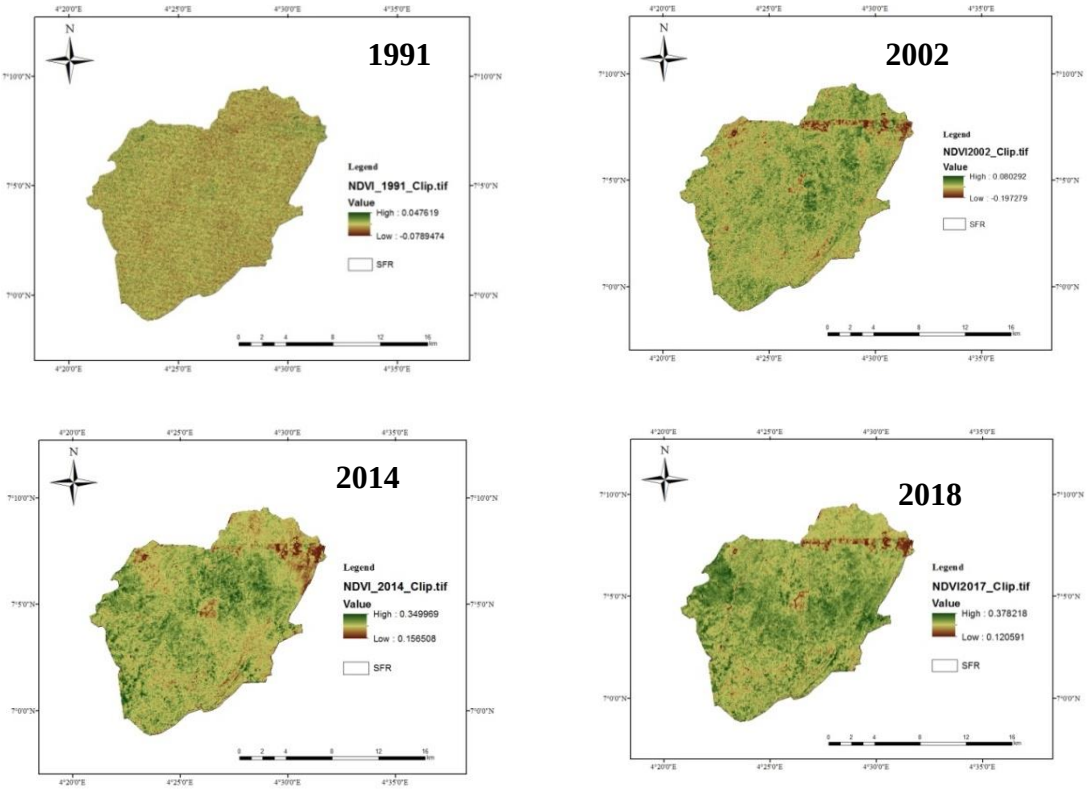

Figure 4: NDVI map of Shasha Forest Reserve

LULC Classification Accuracy Results

The results of the accuracy assessments obtained from random samplings for the classified images showed overall accuracy values of 95.1% (Table 5). User's accuracy ranged between 90.8 and 96.2% while Producer's accuracy values were between 90.8 and 98.1 %. The narrow range of accuracy indicates a less-severe confusion of built-up area with other land-use and land-cover classes. Besides, the high Producer's accuracy values reflect the accuracy of prediction of each of the LULC classes. The User's accuracy reflects the reliability of the classification to the user, and is a more relevant measure of the classification's actual utility on the field. The commission and omission errors were less than 10%, and they reflect the points, which were included in the category while they really did not belong to that category and those omitted in their specific land-use or -cover classes, respectively. The overall Kappa's coefficient for the reserve is 0.9439.

Projected Land-use and Land-cover in Shasha Forest Reserve

Spatial projections of areas under threat of degradation are shown in Figure 5, which depicts the pattern of changes for the LULC types. The projection was set for a period of 12, 22, and 32 years from base year (2018).

Table 5: LULC classification accuracy results

Confusion Matrix					
LULC	Built-up areas	Water bodies/Swamp	Farmland	Forest	Row total
Built-up areas	51	2	0	0	53
Water bodies/Swamp	1	69	6	0	76
Farmland	0	2	59	0	61
Forest	0	0	2	71	73
Column total	52	73	67	71	263
Accuracy assessment result					
LULC	UA	CE	PA	OE	
Built-up areas	96.2	3.8	98.1	1.9	
Water bodies/Swamp	90.8	9.2	93.2	5.5	
Farmland	93.7	6.3	90.8	9.2	
Forest	96.1	3.9	97.3	2.7	
Overall accuracy					95.1
Kappa's coefficient					0.9439

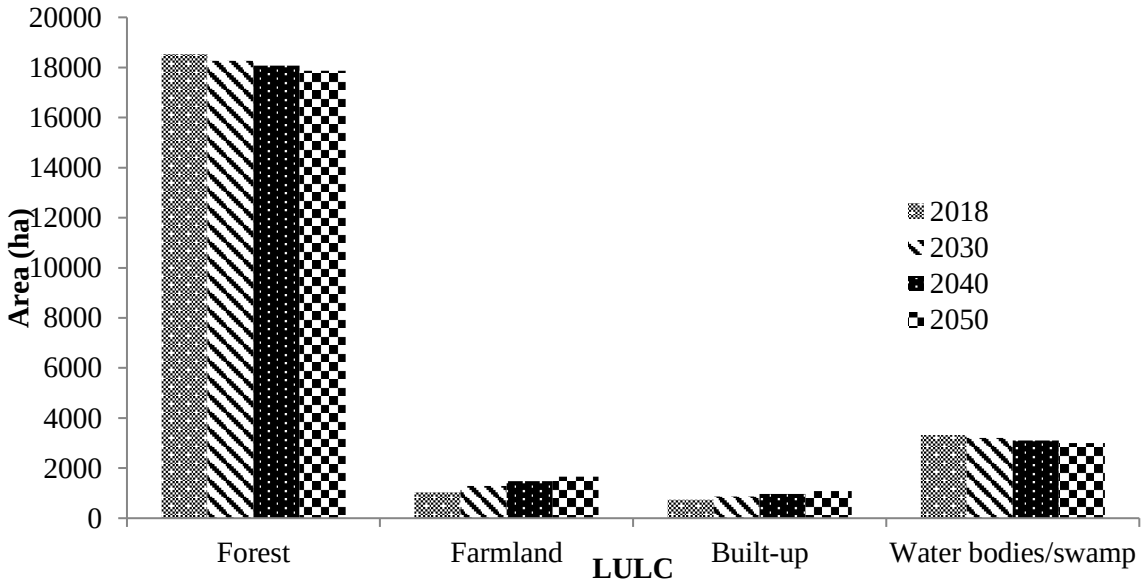

Figure 5: Future projection for the LULC types in Shasha Forest Reserve

DISCUSSION

The serial decline in natural forest and swamps over the 27-year period was observed to result from encroachment and illegal exploitation of timber in the area. It also appears that politics might have played a role in forest decline. For instance, there were gains in forests, and the water bodies/swamps appeared relatively stable between 2002 and 2014. The later four years

of that period corresponds to the first regime of the immediate past governor, who was well-reputed for his outstanding passion for a safe environment and forest. However, the second regime, between 2014 and 2018, was marked by low internally-generated revenue and dwindling economic fortunes of Osun State, where the reserve is situated. Consequently, there were heavy forest encroachment and illegal exploitations in the reserve by unauthorized low-income earners and other civil servants, whose incomes were heavily impacted due to irregular salaries, probably to g*et al*ternative survival means. Other drivers of forest degradation in the area include conversion of forests to farmland for subsistence as well as infrastructural building and roads to connect human settlements to local markets. Adedeji and Adeofun (2014) have reported a trend for the reserve due to perceived conversion of forest to other uses, especially the plantation of exotic timbers such as *Tectona grandis*, *Gmelina arborea* and *Pinus* species. This also corroborates the findings of Adekunle (2006). A large part of the reserve, which was a good repository of plant and animal species, was de-reserved for the establishment of monoculture plantations. Among the factors responsible for the increasing trend of forest plantation in the area was attributed to be their ability to produce high amount of biomass within a relatively short period of time to the detriment of indigenous wood species and losses of valuable biodiversity.

In a study carried out in the study area by Oates *et al*. (2014), it was noted that the decline in natural forest was mostly due to population expansion, rapid urbanization and non-supervision from the concerned authorities such as forest guards with people erecting buildings, de-reserve the reserved area to non-forest uses without checks. Although there was a general increase in the size of the forest plantation between 2002 and 2014, which contributed to forest size within the period, the gains recorded were lost in four years (between 2014 and 2018) with most parts of the plantation being degraded by illegal loggers through serial exploitation of *Gmelina arborea* trees for industrial wood products as a result of low income generation by state government, which further pushed the illegal operators back to forest, ditto for the unpaid government agents, who were expected to protect the forest. Unfortunately, forest conversions have potential consequences on soil conditions, and geomorphology of the area, increase runoff and sedimentation of the river system. Hence, the reduction in the sizes of water bodies/swamps.

Areas once covered by forests are now occupied by either water bodies/swamps, farmland or building infrastructure in 2018 due to population expansion and increasing rate of poverty in the state, which may pose the risk of flooding. This is consistent with the report of Yu and Suganda (2012), who noted that vegetation cover decreases if factors like population expansion exist. The major drivers of forest loss in the area were subsistence agriculture in unauthorized areas and illegal timber exploitations. Farmlands are replacing vegetation cover at a rate too difficult for resilience. There were also signs of illegal timber extractions, which contributed greatly to forest losses during the period.

When simulated, the result showed that if the trend continues, forest and water bodies/swamps would further shrink in sizes beyond the areas they currently occupied, while farmland and built-up areas would claim more of those areas in the forest reserve land in the next few decades, a development inimical to biodiversity and sustainability. Population expansion might mean that more land would be needed to meet food and wood needs of the rural populace in the area, and if not checked, may result in total loss of the reserve within few years. This corroborates the finding of Adubofour (2011), who attributed losses in forest reserve to incessant conversions to other land uses due to rapid and uncontrolled

population growth as well as the need for human survival.

CONCLUSION AND RECOMMENDATIONS

The result has shown that the reserve changed tremendously over 27-year period. The changes resulted in fragmented patches of forest. Consequently, forest covers and water bodies/swamps shrank in extents due to serial and consistent conversions for residential and subsistence agricultural purposes. Large areas were left un-regenerated, thus exposing the lands to further degradations while giving liberty to the subsistence farmers to colonize the fallow area. Hence, farmland and built-up area have become more perennial than forest land-use in the last two decades. It is most likely that forests and water bodies/swamps would decline in extents. Meanwhile, farmlands and built-up areas would rise and claim more land in the near future, possibly denuding the area of appreciable forest cover. This worsens the environmental situation in the area with consequences like losses of vital biodiversity component, siltation of water bodies and the eventual flood disasters, engineered by anthropogenic forces.

It therefore becomes expedient to promote protection of existing natural forest cover to prevent further drains, while considering reliable alternative livelihood means for the forest-dependent people in the interest of sustainability. However, the illegal loggers would need to be handled with tougher measures like arrest and prosecution to serve as deterrent to the potentials dealers. In the case of regeneration and forest management in general, we suggest "plant as you log" measure. For instance, fifty seedlings of same species as those logged could be planted to ensure retainance of natural forest and indigenous species. We discovered that monoculture plantations already mimicked the natural forest during image analyses, reducing species diversity, and this poses the risk of further losses of native species in the near future.

REFERENCES

Adedeji, O. & Adeofun, C.O. 2014. Spatial Pattern of Land Cover Change Using Remotely Sensed Imagery and GIS: A Case Study of Omo-Shasha-Oluwa Forest Reserve, SW Nigeria (1986-2002). Journal of Geographic Information Science 6(4): 375-385.

Adekunle, V.A.J. 2006. Conservation of tree species diversity in tropical rainforest ecosystem of South-west Nigeria. Journal of Tropical Forest Science 18: 91-101.

Adeyemi, A.A. & Adeleke, S.O. 2020. Assessment of Land-cover Changes and Carbon Sequestration Potentials of Trees Species in J4 Section of Omo Forest Reserve, Ogun State, Nigeria. Ife Journal of Science 22(1): 137-152.

Adeyemi, A.A. & Ibrahim, T.M. 2020. Spatiotemporal analysis of land-use and land-cover changes in Kainji Lake National Park, Nigeria. Forestist 70(2): 105-115.

Adubofour, F. 2011. Application of remote Sensing and GIS for Forest cover change Detection. Bsc. Thesis Geodetic Engineering. Kwame Nkrumah University of Science and Technology, Kumasi, Ghana. 111p.

Ayele, G.T., Tebeje, A.K., Demissie, S.S., Belete, M.A., Jemberrie, M.A., Teshome, W.M., Mengistu, D.T. & Teshale, E.Z. 2018. Time Series Land Cover Mapping and Change Detection Analysis Using Geographic Information System and Remote Sensing, Northern Ethiopia. Air, Soil Water Resources 11: 1-18.

Bello, H.O., Ojo, O.I. & Gbadegesin, A.S. 2018. Land Use/Land Cover Change Analysis using Markov-Based Model for

Eleyele Reservoir. Journal of Applied Science Environmental Management 22(12): 1917-1924.

Jiménez, A.A., Vilchez, F.F., González, O.N. & Flores, S.M.L.M. 2018. Analysis of the Land Use and Cover Changes in the Metropolitan Area of Tepic-Xalisco (1973-2015) through Landsat Images. Sustainability 10: 1-15.

Juliev, M., Pulatov, A., Fuchs, S. & Hübl, J. 2019. Analysis of Land Use Land Cover Change Detection of Bostanlik District, Uzbekistan. Polish Journal of Environmental Studies 28(5): 3235-3242.

Kabba, V.T.S. & Li, J. 2011. Analysis of Land Use and Land Cover Changes, and Their Ecological Implications in Wuhan, China. Journal of Geography and Geology 3(1): 104-118.

Li, X., Zhao, S., Yang, H., Cong, D. & Zhang, Z. 2017. A Bi-Band Binary Mask Based Land-Use Change Detection Using Landsat 8 OLI Imagery. Sustainability 9(3): 479-496.

Morgan, R.S., Rahim, I.S. & Abd El-Hady, M. 2015. A Comparison of Classification Techniques for the Land Use/Land Cover Classification. Global Advance Research Journal of Agricultural Science 4(11): 810-818.

Mussa, M., Teka, H. & Mesfin, Y. 2017. Land use/cover change analysis and local community perception towards land cover change in the lowland of Bale rangelands, Southeast Ethiopia. International Journal of Biodiversity Conservation 9(12): 363-372.

Oates, H.I., Isichei, A.O. & Leonov S.E. 2014. Omo Biosphere Reserve, Current Status, Utilization of Biological Resources and Sustainable Management (Nigeria). Working Papers of the South-South Cooperation Programme on Environmentally Sound Socio-Economic Development in the Humid Tropics. UNESCO, Paris. pp. 201-205.

Olokeogun, O.S., Iyiola, O.F. & Iyiola, K. 2014. Application of Remote Sensing and GIS in Land Use/Land Cover Mapping and Change Detection in Shasha Forest Reserve, Nigeria. The International Archives of the Photogrammetry, Remote Sensing and Spatial Information Sciences, Volume XL-8, 2014. ISPRS Technical Commission VIII Symposium, 09-12 December, 2014, Hyderabad, India. pp. 613-616.

Othow, O.O., Gebre, S.L. & Gemeda, D.O. 2017. Analyzing the Rate of Land Use and Land Cover Change and Determining the Causes of Forest Cover Change in Gog District, Gambella Regional State, Ethiopia. Journal of Remote Sensing and GIS 6(4): 1-13.

Thomas, S.C. &MacLellan, J. 2004. Boreal and Temperate Forests, in Forests and Forest Plants. In Encyclopedia of Life Support Systems (EOLSS); UNESCO, Eolss Publishers: Oxford, UK.

Weng, Q. 2002. Land use change analysis in the Zhujiang Delta of China using satellite remote sensing, GIS and stochastic modeling. Journal of Environmental Management 64: 273-284.

Yu, F.T.S. & Suganda, J. 2012. Optical Signal Processing, Computing, and Neutral Networks. John Wiley & Sons, New York. pp. 25-29.

Yuan, F., Sawaya, K.E., Loeffelholz, B.C. & Bauer, M.E. 2005. Land cover classification and change analysis of the Twin Cities (Minnesota) Metropolitan Area by multitemporal Landsat remote sensing. Remote Sensing of the Environment 98: 317-328.